International Journal of GEOMATE, Sept. 2023, Vol. 25, Issue 109, pp.125-132
ISSN: 2186-2982 (P), 2186-2990 (O), Japan, DOI: https://doi.org/10.21660/2023.109.m2312
Geotechnique, Construction Materials and Environment

ADJUSTMENT OF SPEED GOVERNOR FOR MARINE DIESEL GENERATOR ENGINE

* Sergii Gorb[1], Alexey Popovskii[2] and Mykola Budurov[3]

[1,2]Department of Theory of Automatic Control and Computing, National University "Odessa Maritime Academy", Ukraine
[3]Department of Postgraduate and Doctoral Studies, National University "Odessa Maritime Academy", Ukraine

*Corresponding Author, Received: 20 March 2023, Revised: 10 April 2023, Accepted: 9 June 2023

ABSTRACT: The relevance of the work lies in the fact that in the system for engine speed automatic regulation (ESAR) under study, the isodromic speed-regulating governor (SRG) responds differently to disturbances of various sizes due to the presence of two significant non-linearities. The first one is connected with the fact that the oil flow rate through the isodromic needle varies in a power-law dependence of the pressure difference. The second one is related to the deliberate overlap in the pilot valve ports, which prevents the regulator response to disturbances caused by the cyclic operation of the diesel engine and twisting of the camshaft when the pushers of the fuel pumps move to the cams. The purpose of the study is to develop recommendations for optimizing the ESAR of a marine diesel-generator plant with isodromic SRG, considering the disturbances of various magnitudes while ensuring compliance with the requirements of the Classification Society. It has been studied the ESAR of a marine diesel generator manufactured by Yanmar Co., Ltd. of model 6N18AL-UV with isodromic SRG Yanmar NZ61 of the large-capacity tanker "KORO SEA". Its technical supervision is carried out by the Classification Society, the "American Bureau of Shipping" (ABS).

Keywords: Maritime transport; Marine power plant; Internal combustion engine; Automatic control system; Mathematical and computer modelling

1. INTRODUCTION

The Characteristic feature of marine power plants is that the load of marine diesel generator plants at the continuous operational modes of the vessel is 70-80% of the nominal power [1]. The operating conditions of marine auxiliary engines are characterized by step changes in the load [2] due to the on/off of vessel mechanisms, which causes fluctuations of the rotation frequency [3]. The duration of the transition process and the overshoot of regulatory parameters in the transition process are the most significant indicators of the dynamic qualities of a diesel engine [4]. The international standard ISO 3046-4:2009 determines that the limit values of these indicators are regulated by the supervisory organizations in the Rules for the Classification and Construction of Sea-Going Ships [5]. The maximum allowable control time for marine diesel generators with full instantaneous load shedding is 5 s with an overshoot of 10%. The frequency should return within ± 1% of the final steady state in no more than 5 s [6].

To optimize the SRG parameters, mathematical modelling can be used [7]. Its use is facilitated by the developed methods for the detailed calculation of centrifugal frequency meters and hydraulic systems [8]. The oil flow rate through the needle of isodromic feedback (FB) has a power-law dependence on the pressure difference [9], which can change several times, while the pressure difference at the pilot valve port and the throttle opening of the cavity of isodromic belt change insignificantly. Change in the pressure difference leads to a change of isodromic time, and therefore the SRG frequency characteristics change [10]. The non-linearity associated with the deliberate overlap in the pilot valve ports prevents the regulator response to disturbances caused by the cyclic operation of the diesel engine and the twisting of the camshaft. Due to this, ESAR with isodromic SRG response differently to disturbances of various magnitudes [11].

This work developed recommendations to improve the operation of isodromic SRG of auxiliary engines, considering the disturbances of various sizes and simultaneously meeting the requirements of the Classification Society.

2. MATERIALS AND METHODS

The study was carried out using the ESAR model [12], according to which the diesel engine torque is in the relative variables:

$$\boldsymbol{\overline{M}_d = \frac{1}{\eta_{m0}}[\overline{M}_i - (1-\eta_{m0})(0.19 + 0.14\overline{M}_i + 0.67\overline{\omega}_d)]} \quad (1)$$

where $\boldsymbol{\eta_{m0}}$ is the mechanical efficiency of the diesel engine in the nominal mode; $\boldsymbol{\overline{M}_i}$ is the relative indicator moment of diesel engine; ¯ω_d is the relative angular velocity of the shaft.

The indicator moment of a diesel engine is considered to be proportional to the rack travel of the fuel pumps ($\overline{\boldsymbol{M}}_i = \overline{\boldsymbol{h}}_r$). Due to the cyclic operation of the diesel engine, the operation of value assignment $\overline{\boldsymbol{h}}_r$ of the variable $\overline{\boldsymbol{M}}_i$ is performed within time intervals Δτ (s) [13]:

$$\Delta\tau = \frac{\varphi_c}{i n_{d0} \overline{\omega}_{d0} \cdot 60} \qquad (2)$$

Where: $\boldsymbol{\varphi_c}$ is the angle of crank rotation per cycle, deg; i is the number of cylinders in the diesel engine; $\boldsymbol{n_{d0}}$ is the shaft rotation frequency in nominal mode, $\min^{-1}$.

Diesel engines are characterized by a delay in the change $\overline{\boldsymbol{M}}_i$ in relation to the rack travel of the fuel pumps $\overline{\boldsymbol{h}}_r$ [14]:

$$\tau_{del} = \frac{20-10\overline{h}_r}{6 n_{d0} \overline{\omega}_d} \qquad (3)$$

The relative change in the fuel supply is related to the SRG output signal by the ratio:

$$\overline{h}_r{}' = \frac{\overline{z}_p}{k_{u.m}} \qquad (4)$$

Where: $\overline{\boldsymbol{z}}_p$ is the relative value of the stroke of operating mechanism; $\boldsymbol{k_{u.m}}$ is the relative value of stroke usage.

Diesel-generator plant of Yanmar 6N18AL-UV model with isodromic regulator Yanmar NZ61 of the large-capacity oil tanker "KORO SEA" was selected as the object of the study. This oil tanker was built at the shipyard Namura Ship Building Co. Ltd. in Japan and put into operation on February 27, 2008. Yanmar 6N18AL-UV engine develops a nominal capacity of 500 kW and a nominal rotation frequency of 900 $\min^{-1}$, it is a four-stroke, medium-speed, trunk piston with direct injection, six-cylinder, non-reversible. It has an impulse pressure air charging system, which is provided by the turbocharger of the IHI RH133 model [15]. Also, the Yanmar 6N18AL-UV diesel engine with a turbocharger of the IHI RH133 model operates in tandem with an alternator made by Taiyo Electric Co., Ltd. FE547A-8 model. Its technical characteristics are taken from technical documentation [15]. Yanmar 6N18AL-UV is equipped with Yanmar Co., Ltd. model NZ61 SRG [16]. It is shown the schematic diagram of the Yanmar NZ61 regulator without limiting mechanisms, speed droop and speed setting mechanism (Fig. 1).

3. RESEARCH SIGNIFICANCE

The findings of the study provide valuable insights for engineers and researchers working in the field of esar and marine diesel-generator plants, ultimately leading to improved system reliability and stability. The research provides valuable insights into the technical and operational aspects of marine diesel generators and their speed regulation systems. It can help improve the performance and efficiency of marine diesel generators, reduce fuel consumption and emissions, and increase the safety and reliability of marine operations. Moreover, the research can serve as a reference and guide for future studies in the field of marine engineering and power generation.

4. RESULTS AND DISCUSSION

The equations of mass balance in the cavity of the servomotor, the balance of forces on the isodrom piston and the motion of the power piston:

$$f_i \frac{dz_i}{dt} = \frac{dQ_{pv}}{dt} - \frac{dQ_{rv}}{dt} - f_m \frac{dz_p}{dt} \qquad (5)$$

$$(p_2 - p_1) f_i = \sigma_i z_i \qquad (6)$$

$$\frac{dz_p}{dt} = \frac{1}{f_m + f_b} \frac{dQ_{pv}}{dt} \qquad (7)$$

Where: $\boldsymbol{f_i}$, $\boldsymbol{f_m}$ and $\boldsymbol{f_b}$ are the areas of the isodrom piston, middle and lower surfaces of the power piston; $\boldsymbol{z}_i$ and $\boldsymbol{z_p}$ is the stroke of the isodrom piston and power piston; $\boldsymbol{t}$ – time; $\boldsymbol{Q_{pv}}$ and $\boldsymbol{Q_{rv}}$ – the amount of oil that has passed through the pilot valve ports and needle valve; p_2 and p_1 – pressure before and after the needle valve; $\boldsymbol{\sigma_i}$ is the total rigidity of springs of the isodrom piston.

The oil flow through the throttle is determined by the equation of outflow for a section with sharp edges:

$$\frac{dQ_{rv}}{dt} = \mu_{rv} f_{rv} \sqrt{\frac{2|p_2 - p_1|}{\rho_o}} \qquad (8)$$

Where: $\boldsymbol{\mu_{rv}}$ is the flow coefficient of the flow cross-section of throttle; $\boldsymbol{f_{rv}}$ is the area of the flow cross-section of throttle; $\boldsymbol{\rho_o}$ is the oil density.

Substituting expressions (7; 8) into equation (5), it is expected to receive the following:

$$f_i \frac{dz_i}{dt} = (f_m + f_b) \frac{dz_p}{dt} - (p_2 - p_1) \mu_{rv} f_{rv} \sqrt{\frac{2}{|p_2 - p_1| \rho_o}} - f_m \frac{dz_p}{dt} \qquad (9)$$

After simplifications considering the expression (6):

$$z_i \left(p f_i + \frac{\sigma_i \mu_{rv} f_{rv}}{f_i} \right) \sqrt{\frac{2}{|p_2 - p_1| \rho_o}} = p z_p f_b \qquad (10)$$

The transfer function of the isodromic FB is determined by the ratio of the relative force on the belt to the relative stroke of the power servomotor:

$$W_i = \frac{(p_2 - p_1) f_{s.p} z_{p.o}}{F_{c.o} z_p} \qquad (11)$$

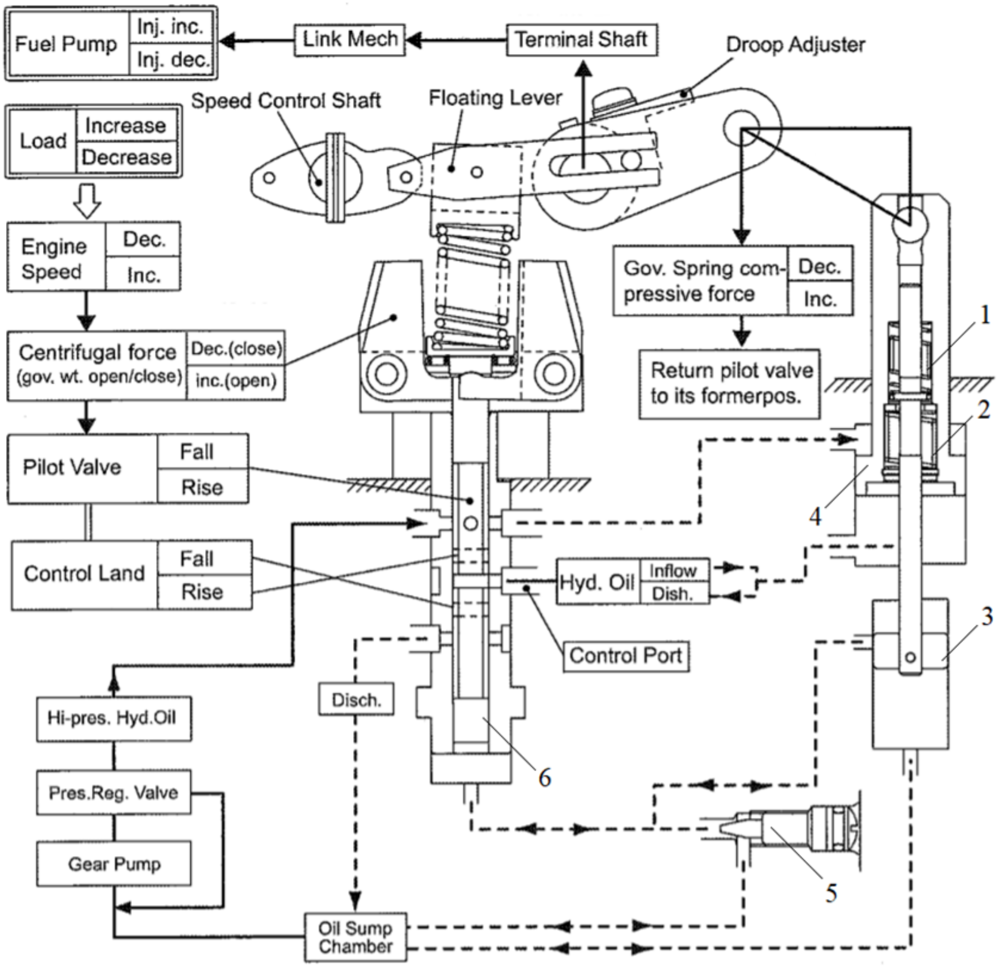

Fig. 1 Schematic diagram of the Yanmar NZ61 regulator

Note: 1 – upper spring; 2 –lower spring; 3 – isodrom; 4 – power piston; 5 – needle valve; 6 – oil sump

Where: $f_{s.p}$ is the area of belt of the isodromic FB in the pilot valve; $z_{p.o}$ is a full stroke of the power servomotor; $F_{c.o}$ is centrifugal force of loads at the nominal rotation frequency of the drive roller.

Substituting expressions (6; 9; 10) into equation (11), it is expected to receive the following:

$$W_i = \frac{\sigma_i f_{s.p} f_b z_{p.o}}{f_i^2 F_{c.o}} \frac{p}{p+\frac{\sigma_i \mu_{rv} f_{rv}}{f_i^2}\sqrt{\frac{2}{|p_2-p_1|\rho_o}}} \tag{12}$$

Let's introduce the designation for the transfer coefficient and time of the isodromic feedback:

$$k_i = \frac{\sigma_i f_{s.p} f_b z_{p.o}}{f_i^2 F_{c.o}} \tag{13}$$

$$T_i = \frac{f_i^2}{\sigma_i \mu_{rv} f_{rv}}\sqrt{\frac{|p_2-p_1|\rho_o}{2}} \tag{14}$$

Then the transfer function will take the form adopted in the theory of automatic control:

$$W_i = \frac{k_i T_i \mathrm{p}}{T_i \mathrm{p}+1} \tag{15}$$

According to the expressions (12-14), the time of isodromic FB T_i depends on the pressure difference $p_2 - p_1$ on the needle valve. The time averaging of isodromic FB is possible only in relation to a specific disturbing effect, since the pressure difference $p_2 - p_1$ changes significantly. It is proposed to use a non-linear model of isodromic FB, the time of isodromic FB is expressed through its relative output signal:

$$\overline{\xi_1} = \frac{(p_2-p_1) f_{s.p}}{F_{c.o}} \tag{16}$$

In this case:

$$T_i = \frac{f_i^2}{\sigma_i \mu_{rv} f_{rv}}\sqrt{\frac{F_{c.o}\rho_o}{2 f_{s.p}}}\sqrt{|\overline{\xi_1}|} = T_i^* \sqrt{|\overline{\xi_1}|} \tag{17}$$

and the value T_i^* (which is constant) is specified in the initial data. The calculation expression of the isodromic FB takes the form:

$$W_i' = \frac{\sigma_i z_i z_{p.o}}{F_{c.o} z_p} \tag{19}$$

Let's substitute the value z_p into expression (19):

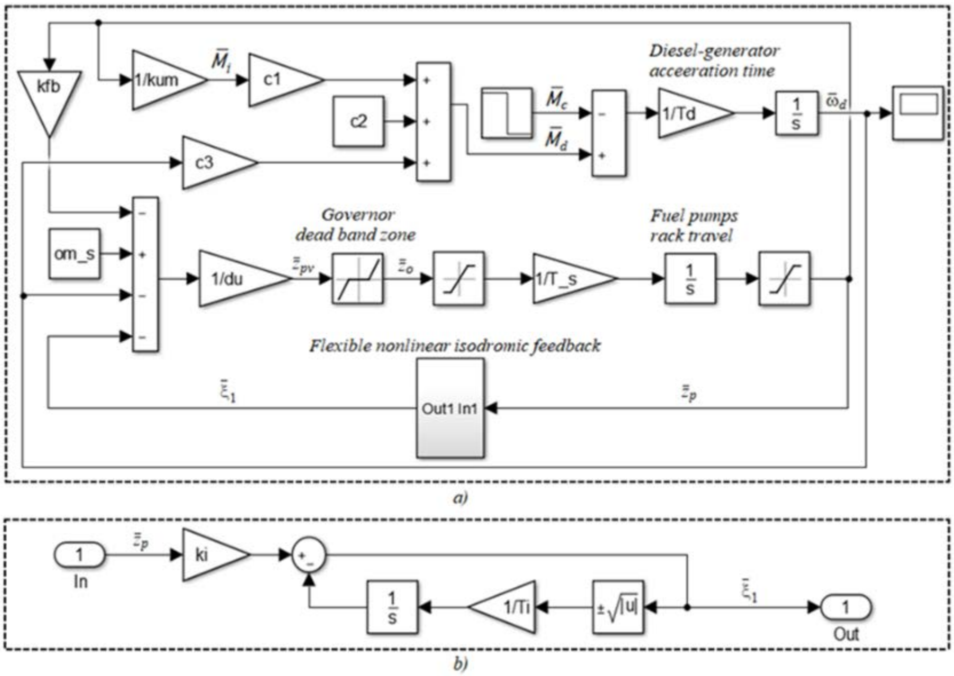

Fig. 2 ESAR model of the Yanmar 6N18AL-UV marine diesel generator set with the Yanmar NZ61 regulator
Note: a - simulation scheme; b – non-linear isodromic FB, formed by expression (18).

$$\boldsymbol{f_i z_i = f_g z_p k_{p.g} - Q_{rv}}, \tag{20}$$

where: $\boldsymbol{f_g}$ is the area of the isodromic feeding plunger; $\boldsymbol{k_{p.g}}$ is transfer coefficient from the power piston to the isodromic feeding plunger.

Then, considering the equation (6) and expression (8), it is expected to receive the following:

$$\boldsymbol{W_i'} = \frac{\sigma_i f_g k_{p.g} z_{p.o}}{f_i F_{c.o}} \frac{p}{p + \frac{\sigma_i \mu_{rv} f_{rv}}{f_i^2}\sqrt{\frac{2}{|p_2 - p_1|\rho_o}}}. \tag{21}$$

Transfer coefficient of isodromic FB is:

$$\boldsymbol{k_i}' = \frac{\sigma_i f_g k_{p.g} z_{p.o}}{f_i F_{c.o}}. \tag{22}$$

To further investigate the performance of the ESAR system in various operating modes, it was necessary to analyze the magnitudes of disturbances that arise from the on/off switching of consumers with power over 30 kW. The total load of operating diesel generators was evaluated. The largest values of load shedding on the large-capacity tanker "KORO SEA" are: normal operating mode of the vessel – 25-50%; cleaning of cargo tanks while a vessel is moving – 20-55%; cargo heating while the vessel is moving – 10-30%; when a vessel enters/leaves port(s) – 25-60%; during cargo operations – 25-75%; in port – 20-40%.

Disturbances on the system are applied through the load channel by changing the relative moment of resistance M_c. The angular coefficient of the load characteristic is 0.044 rel. units. When choosing the values of setting parameters of the ESAR of the diesel generator, the overshoot of rotation speed was minimized while limiting the control time in the transition process. ESAR model of the Yanmar 6N18AL-UV marine diesel with Yanmar NZ61 regulator (Figure 2).

The following values were used in the simulation: initial $\boldsymbol{M_{c1}}$ and final $\boldsymbol{M_{c2}}$ values of the relative load moment 0…1 rel. unit; relative rotation frequency in the initial mode $\boldsymbol{\overline{\omega}_d = 1 + (1 - M_{c1})k}$, where k = 0.044 rel. units − angular coefficient of the load characteristic; diesel generator acceleration time $\boldsymbol{T_d}$ = 1.8 s; relative value of the governor dead zone to the signal $\boldsymbol{\overline{\omega}\ \varepsilon}$ = 0.002 rel. units; non-uniformity of the rotation frequency meter $\boldsymbol{\delta_u}$ = 0.08 rel. units; transfer coefficient of isodromic FB $\boldsymbol{k_i}$ = 0.05 ... 0.5 s^{-1}; isodromic FB time $\boldsymbol{T_i}^*$ = 0.1 ... 3 s; time of the power servomotor SRG $\boldsymbol{T_s}$ = 0.36 s; utilization factor of the regulator stroke during the transition from zero to nominal fuel supply $\boldsymbol{k_{u.m}}$ = 0.75 rel. units; speed droop coefficient $\boldsymbol{k_{f.b}}$ = 0.067 rel. units; mechanical efficiency of diesel generator $\boldsymbol{\eta_{m0}}$ = 0.87 rel. units; angle of rotation of the crank per cycle $\varphi_c = 4\pi$; number of engine cylinders i = 6; shaft rotation frequency in the nominal mode n_{d0} = 900 min^{-1}; $\boldsymbol{c_1 = (1 - 0.14(1 - \eta_{m0}))/\eta_{m0}}$; $\boldsymbol{c_2 = -0.19(1 - \eta_{m0})/\eta_{m0}}$; $\boldsymbol{c_3 = -0.67(1 - \eta_{m0})/\eta_{m0}}$; the initial position of the rod of the control power hydraulic cylinder $\boldsymbol{z_p = (1 - c_3\overline{\omega}_d - c_2)k_{u.m}/c_1}$; speed setting value $\boldsymbol{\overline{\omega}_s = \overline{\omega}_d + k_{f.b} z_p}$.

Figures 3-7 show the transition processes for the case of resetting these values. Through the analysis of transition processes, engineers can identify potential issues and take appropriate measures to ensure system reliability and stability. In a non-optimal operating condition is when the ESAR system operates at less than full capacity, which can occur due to changes in the system's load or other external factors. In this scenario, the ESAR system may not be able to fully capture and recover the energy that it is designed to.

While shedding mode can improve the efficiency of the system, it may not be the best solution in all cases, particularly when the system is operating at lower capacities. The behavior of the ESAR system under non-optimal conditions can be significantly different from that observed in shedding mode (Figure 7). This setting practically retains the overshoot of rotation frequency shown in Figure 3 at 25% load shedding, and compared to the optimal settings of the isodromic feedback, it worsens overshoots at 50% load shedding by no more than 0.01 rel. units, and when shedding 75% of the load – no more than 0.03 rel. units. However, in operation, there is no possibility of reconfiguring the isodromic FB, depending on the operating mode of the vessel. It is proposed to use the concept of "suboptimal setting" of the isodromic FB of ESAR. For such a value, the suboptimal setting of the isodromic FB is $k_i = 0.05$ s^{-1} and $T_i = 0.4$ s.

The transition processes in ESAR of the Yanmar 6N18AL-UV marine diesel generator with a Yanmar NZ61 regulator are shown at 25%, 50% and 75% load shedding with a suboptimal setting of isodromic feedback. With a 100% load shedding, the control time amounted to 2.4 s with a relative overshoot of rotation frequency of 0.05 rel. units. It was compared the calculated values of the quality indicators with the experimental ones for three load shedding/surge options (Table 1).

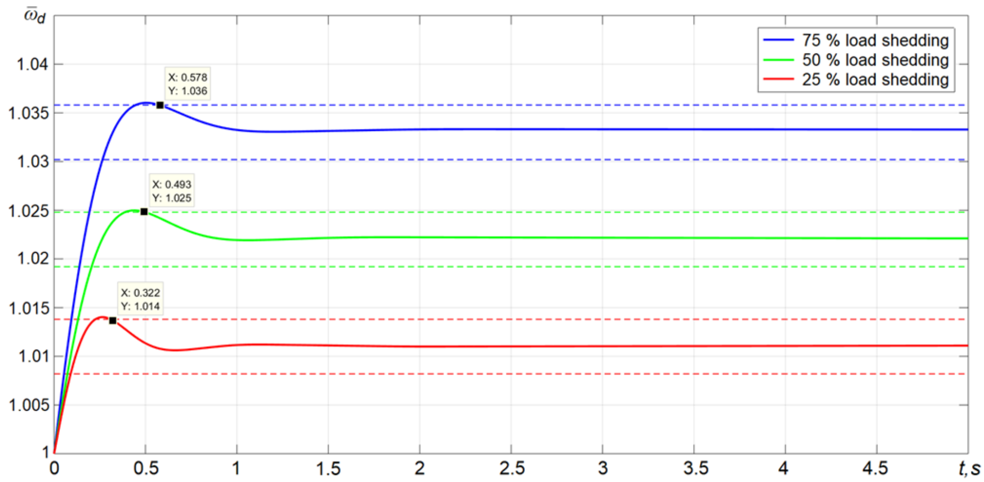

Fig. 3 Transition processes in ESAR at 25%, 50% and 75% load shedding

Note: 25 % ($k_i = 0.05$ s^{-1}; $T_i = 0.3$ s); 50 % ($k_i = 0.1$ s^{-1}; $T_i = 0.4$ s); 75 % ($k_i = 0.2$ s^{-1}; $T_i = 0.6$ s).

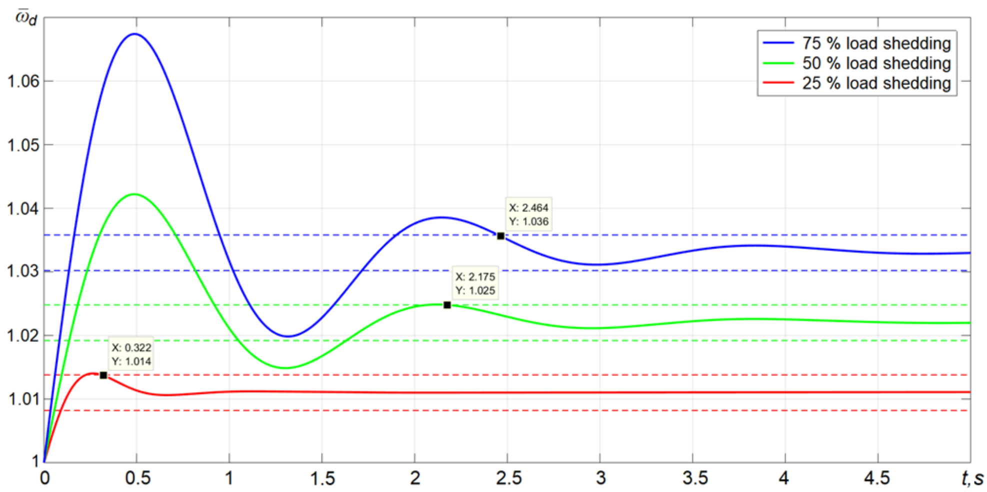

Fig. 4 Transition processes in ESAR with the optimal isodromic FB setting for the 25% shedding mode

Note: (ki = 0.05 s-1; Ti = 0.3 s).

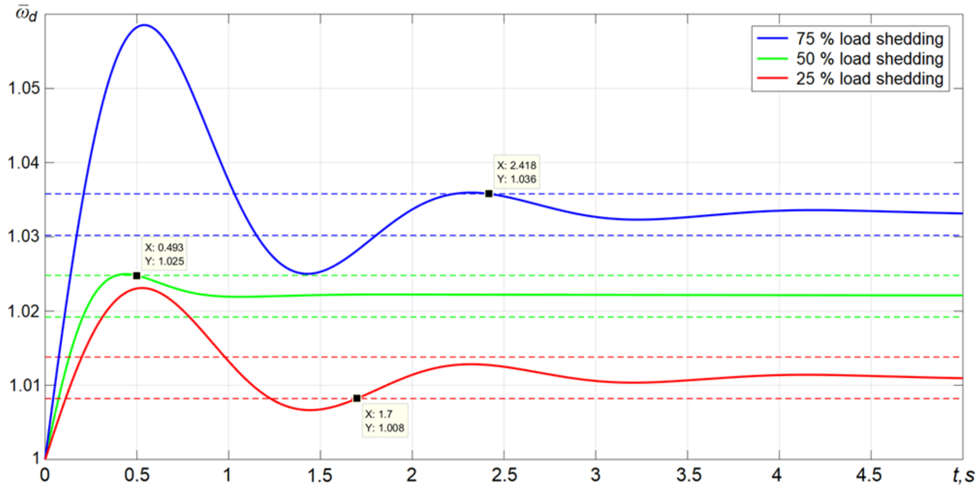

Fig. 5 Transition processes in ESAR with the optimal isodromic FB setting for the 50% shedding mode
Note: ($k_i = 0.1\ s^{-1}$; $T_i = 0.4\ s$).

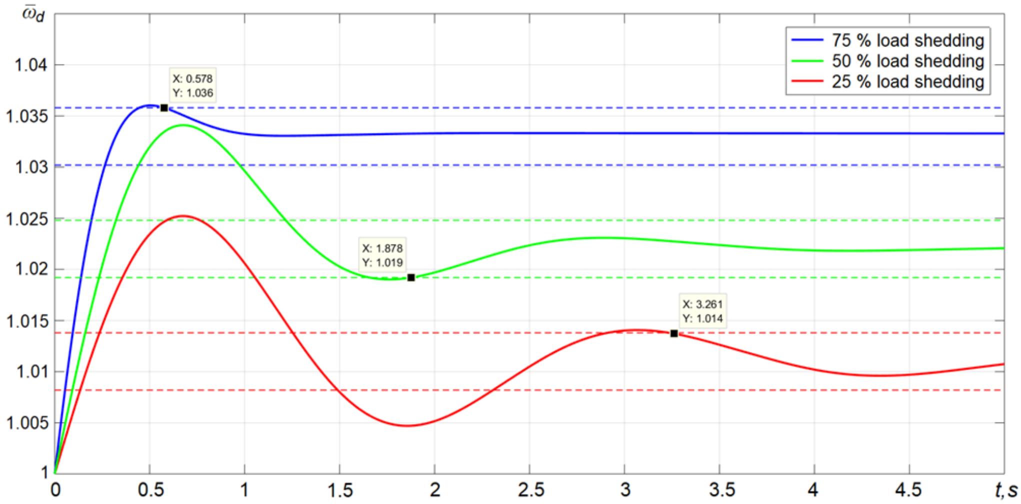

Fig. 6 Transition processes in ESAR with the optimal isodromic FB setting for the 75% shedding mode
Note:($k_i = 0.2\ s^{-1}$; $T_i = 0.6\ s$).

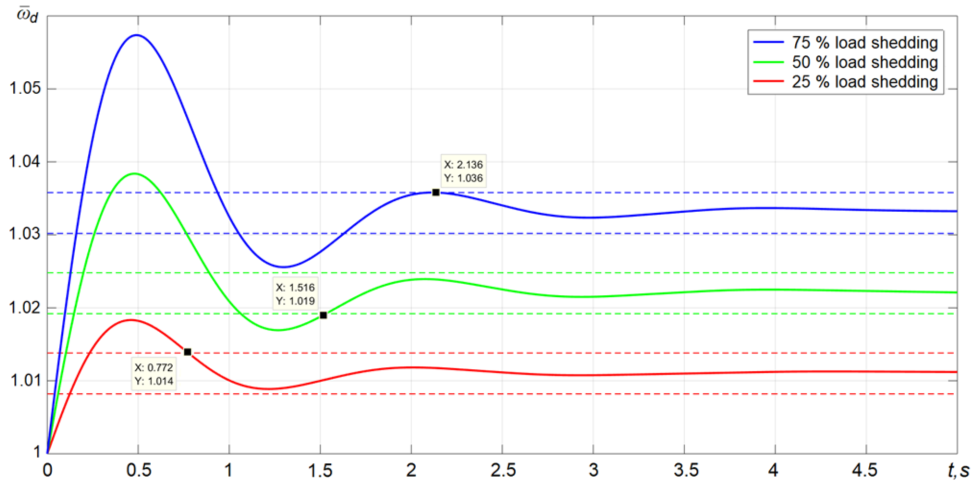

Fig. 7 Transition processes in ESAR with suboptimal setting of isodromic FB for the most probable cases of load shedding
Note:($k_i = 0.05\ s^{-1}$; $T_i = 0.4\ s$).

Table 1. Experimental and calculated values of quality indicators

Load change, %	Experiment				Calculations			
	Shaft speed of diesel generator, min^{-1}			Regulation time, s	Shaft speed of diesel generator, min^{-1}			Regulation time, s
	Before transition process	Transition process	Steady-state mode		Before transition process	Transition process	Steady-state mode	
100 → 0	900	955	940	2.8	900	945.2	937.5	2.4
0 → 50	940	905	920	3.4	940	912.5	922.5	3.1
50 →100	920	880	900	4.1	920	888.6	897.5	3.8

The use of suboptimal setting that is focused on the most probable operational disturbances leads to an improvement in the main characteristics of transition process even in a well-established ESAR operation.

The quality and efficiency of vessels' ESAR are the topical issues in the field of engine manufacturing. F. Nitsch, M. Deissenroth-Uhrig, C. Schimeczek and V. Bertsch [17] determined that high-quality automatic regulation of the rotation frequency of diesel shaft is due to the nature of the ESAR transition process and it is provided by adjusting the controller for the most probable operational disturbance. According to C. Ma, E.Z. Song, Y. Long and C. Yao [18], the tasks of designing and modelling systems of parametric settings are solved at a new qualitative level. An increase of the professional level of training of the vessel's crew is also considered. A tendency to ensure simultaneous and continuous monitoring and diagnostics of the technical state in the power plants of vessels with modern systems of automation and control is observed [19].

A continuous process of collecting and analyzing information about the value of diagnostic parameters of the object state should be carried out. Complex technical systems and tools provide reliable values of the parameters under study.

A.J. Mahdi and B.A. Fadheel [20] showed that the non-linearities of SRG when optimizing the ship power plant provide good dynamics of diesel under the conditions of step disturbances specific to the operating modes. At the same time, the creation of an effective energy mode for generating electricity occurs when the value of the adjustable parameter of the diesel engine is commensurate with the size of the generator's electric load. To improve the efficiency of the diesel generator set, it is necessary to consider the fact that ESAR in operation should provide the dynamics required by the Classification Society in a wide range of load-shedding/surge [21].

K. Tokumitsu, H. Amano and K. Kawabe [22] determined that there is a tendency to increase the use of electromotive systems in water transport, which are supported by the power plant of autonomous vessels driven by internal combustion engines. This increases the reliability of the power system. In accordance with the recommendations of the resolution Marine Environment Protection Committee (MEPC) 77 [23-25], it is necessary to increase funding for research on the optimization of existing ESAR of marine diesel engines to improve the energy efficiency of the merchant fleet.

5. CONCLUSIONS

To optimize operation under the most probable step change of load in normal operation, a joint analysis of the duration of the vessel's operating modes and the most probable values of load shedding/surge in each operational mode was conducted. The proposed mathematical model of ESAR of a marine diesel generator set allowed for analyzing the transition processes for the most probable cases of load changes.

The methodology was tested on the Yanmar 6N18AL-UV marine diesel generator set with Yanmar NZ61 isodromic regulator and it ensured the fulfilment of the transition process characteristics regulated by the ABS Classification Society in all transition modes. It is shown the possibility to provide the following overshoots of rotation frequency during the load shedding/surge by means of optimizing the setting: 25% – no more than 0.005 rel. units;50% – overshoots no more than 0.01 rel. units; 75% increase in overshoots no more than 0.025 rel. units.

Formulated methodology for selecting the SRG setting parameters made it possible to optimize the operation of ESAR for the actual operating conditions of the diesel generator. Further research is planned in the direction of evaluating the feasibility of automatization of the change in SRG setting parameters, depending on the value of actual indicators of the change in rotation frequency of the diesel generator and the output signal of SRG.

6. REFERENCES

[1] Kamkin S. V., and Shmelev A. V., Diesel power plants. Completing auxiliary mechanisms and equipment, heat utilization and efficiency determination, Moscow: Mortechinformreklama, 1984, pp 1-50.

[2] Dimopoulos G. G., Kougioufas A. V., and Frangopoulos C. A., Synthesis, design and operation optimization of a marine energy system, Energy, Vol. 33, Issue 2, 2008, pp.180-188.

[3] Giannoutsos S. V., and Manias S. N., Energy management and D/G fuel consumption optimization in the power system of marine vessels through VFD-based process flow control, In: 15th International Conference on Environment and Electrical Engineering (pp. 842-850), Rome: IEEE, 2015.

[4] Belyaev M. E., Gerasimov D. N., Rymalis M. R., and Semenov S. A., Design of Diesel Engine Mathematical Model Oriented to Speed Control, Journal of Computer and Systems Sciences International, Vol. 57, 2018, pp. 626-639.

[5] ISO 3046-4:2009. 2009. Reciprocating internal combustion engines, Performance. Part 4: Speed governing, 2009, Retrieved from https://www.iso.org/standard/44318.html.

[6] American Bureau of Shipping Rules for Building and Classing Marine Vessels, 2022, Retrieved from https://ww2.eagle.org/en/rules-and-resources.html?gclid=EAIaIQobChMIipGahpCb QIVB6p3Ch3DugGMEAAYASAAEgLQtPD_BwE.

[7] Solem S., Fagerholt K., Erikstad S. O., and Patricksson O, Optimization of diesel electric machinery system configuration in conceptual ship design, Journal of Marine Science and Technology, Vol. 20, 2015, pp. 406-416.

[8] Gorb S. I., Mathematical model and analysis of the dynamics of the hydromechanical speed regulator, Dvyhatelestroenye, 2, 1988, pp. 31-33.

[9] Chen H. F., Cheng D. Z., and Zhang J. F., Nonlinear design methods for control systems, In: Proceedings of the14th IFAC World Congress (pp.521-526), Kidlington: Elsevier, 1999.

[10] Greve M., Engine Control with Open Software Based on an Industrial PLC, MTZ Industrial, Vol. 6, 2016, pp. 46-55.

[11] Machowski J., Bialek J. W., and Bumby J. R., Power system dynamics and stability, Chichester: Wiley, 1997, pp. 1-888.

[12] Gorb S. I., Analysis of systems of automatic regulation of the frequency of rotation of marine diesel installations, Moscow: Mortechinformreklama, 1989, pp. 1-44.

[13] Gorb S. I., and Budurov M. I., Optimization of an automatic control speed of a marine diesel engine, Automation of ship technical facilities: science and technology, Vol. 27, 2021, pp. 3-21.

[14] Gorb S. I., Modelling of the dynamics of the work of diesel propulsion plants on the ECM, Moscow: Mortechinformreklama, 1986,pp. 1-48.

[15] Finished Plan for Main Diesel Generator Engine 6N18AL-UV, I.B.C. No. B6-0046501, 2008, Retrieved from https://www.yanmar.com/global/marinecommercial/products/auxiliary_engine/6ey18alw/.

[16] Service Manual for NZ61/NZ115 Series Hydraulic Governor, I.B.C. No. 42221-997031, 2022, Retrieved from https://www.yanmar.com/media/news/2020/08/14010555/medium_speed_engines_full_en.pdf.

[17] Nitsch F., Deissenroth-Uhrig M., Schimeczek C., and Bertsch V., Economic evaluation of battery storage systems bidding on day-ahead and automatic frequency restoration reserves markets, Applied Energy, Vol. 298, 2021, article number: 117267.

[18] Ma C., Song E. Z., Long Y., and Yao C., Research on Adaptive Speed Control of Marine Diesel Engine based on Discrete Time Integral Minimal Control Synthesis, In: 2021 China Automation Congress (pp. 803-807), Rome: IEEE, 2021.

[19] Abbas M. K., Hassan Q., Jaszczur M., Al-Sagar Z. S., Hussain A. N., Hasan A., and Mohamad A. Energy visibility of a modeled photovoltaic/diesel generator set connected to the grid, Energy Harvesting and Systems, Vol. 9, Issue 1, 2021, pp. 27-38.

[20] Mahdi A. J., and Fadheel B. A., A modified algorithm for economic evaluation between diesel-generator and pv solar system, In: *2018 2nd International Conference for Engineering, Technology and Sciences of Al-Kitab* (pp. 83-87), Rome: IEEE, 2018.

[21] Bevrani H., Golpira H., Messina A. R., Hatziargyriou N., Milano F., and Ise T., Power system frequency control: An updated review of current solutions and new challenges, Electric Power Systems Research, Vol. 194, 2021, article number: 107114.

[22] Tokumitsu K., Amano H., and Kawabe K., Improved load frequency controller for reduction of both area control error and automatic frequency restoration reserve energy cost, *Madrid PowerTech* (pp.1-6), Rome: IEEE, 2021.

[23] Marine Environment Protection Committee (MEPC) 77, 2021, Retrieved from https://www.imo.org/en/MediaCentre/MeetingSummaries/Pages/MEPC77.aspx

[24] Chomphan, S., Investigation on Vibration and Sound Signals from Hybrid-Engine to Electric Vehicles, International Journal of GEOMATE, vol. 24, no. 104, 2023, pp. 77–84.

[25] Wagino, E. A., Bahrul A., and Afnison, W., Electric Turbo Compounding (Etc) As Exhaust Energy Recovery System on Vehicle, International Journal of GEOMATE, vol. 19, no. 71, (2020), pp. 228–234.